Generalized Wireless Network Coding Schemes for Multi-Hop Two-Way Relay Channels

Gengkun Wang, Wei Xiang, *Senior Member, IEEE*, and Jinhong Yuan, *Senior Member, IEEE*

***Abstract*—Due to the overwhelming complexity of multi-hop transmission and inter-message interference, only a limited amount of research has been carried out in the implementation of wireless network coding (WNC) for generalized multi-hop two-way relay channels (MH-TRCs), let alone the generalization of multi-hop wireless network coding (MH-WNC) schemes. Our recent work showed that the MH-WNC scheme with fixed two transmission time intervals was unable to always outperform conventional Non-NC schemes in outage performance for the MH-TRC with an arbitrary number of nodes. In view of this fact, a generalized MH-WNC scheme with multiple transmission time intervals (TTIs) is designed for the L-node K-message MH-TRC in this paper. Closed-form expressions for the upper bound of the outage probability for two prominent relaying network coding strategies (i.e., analog network coding and compute-and-forward network coding) are derived. Moreover, by investigating the relationships between the outage probability and the numbers of nodes, messages and TTIs, we obtain an optimal MH-WNC scheme which can achieve the best outage probability and always outperform Non-NC in the MH-TRC with an arbitrary number of nodes.**

***Index Terms*—Multi-hop wireless network coding, multi-hop two-way relay channels, outage probability, analog network coding, compute-and-forward network coding.**

I. Introduction

MULTI-HOP networks, such as wireless sensor networks [1], wireless mesh networks [2], mobile ad hoc networks [3], vehicular ad hoc networks [4], have emerged as promising approaches to provide more convenient wireless communications due to their extended coverage, easy deployment and low costs. However, multi-hop wireless relay communications require an increase number of time slots to transmit data in a multi-hop manner [5] [6]. Information is conveyed through a series of intermediate relays in a conventional hop-by-hop and message-by-message manner, which limits network throughput, and thus the data rate of the system. The advent of network coding (NC) has offered a new opportunity to improve network throughput and reliability by exploiting interference in intermediate relays [7].

Combined with network coding and self-information cancelation, wireless network coding (WNC) for two-way relay channels (TWRCs) has come to the forefront [8] [9]. There is a large body of work on the implementation and performance analyse (including outage probability, bit-error-rate and sum-rate) of WNC in the TWRC [10]–[12]. Subsequent work in extending WNC to multi-hop two-way relay channels (MH-TRC) soon followed. Zhang *et al.* [8] described physical-layer network coding (PNC) for general uni-directional and bi-directional linear networks, which can achieve the upper-bound capacity of 0.5 frame/time slot in each direction for bi-directional transmissions between two end nodes [13]. However, there is no performance analyse presented in this paper. More recently, You *et al.* applied analog network coding (ANC) to the MH-TRC in [14] [15], where the proposed AF-ANC-Central and AF-ANC-Even schemes can improve the network throughput compared to Non-NC schemes. However, there is no work on a generalized ANC transmission scheme for the MH-TRC with an arbitrary number of hops (referred to as all-scale MH-TRCs), and there is no published work on outage performance for such generalized MH-TRC networks, either.

Our previous work [16] [17] generalized the multi-hop wireless network coding (MH-WNC) scheme with fixed two transmission time intervals (TTIs) (referred to as 2-TTI MH-WNC) for the L-node K-message MH-TRC. The 2-TTI MH-WNC scheme was proven to markedly improve the spectral efficiency over conventional Non-NC schemes. However, it was also shown that the 2-TTI MH-WNC scheme is unable to outperform Non-NC for all-scale MH-TRCs. The multi-hop analog network coding (MH-ANC) scheme [16] can only outperform Non-NC in the MH-TRC with a small number of nodes, while the multi-hop compute-and-forward (MH-CPF) scheme [17] has better outage performance than Non-NC only for the MH-TRC with a large number of nodes.

Due to the overwhelming complexity of multi-hop transmission and inter-message interference, there has not been a great deal of work in the literature on the implementation and performance analyse of WNC in the MH-TRC, let alone generalized WNC schemes for the MH-TRC. In view of this fact, this paper aims to fill the research gap by proposing a generalized WNC scheme with multiple TTIs (referred to as I-TTI MH-WNC), which is a generalized scheme for the 2-TTI MH-WNC scheme in [8] [14], [16]–[19]. The key idea of this research is to investigate the relationships between the outage probability and the numbers of nodes, messages and TTIs, then devise an optimal MH-WNC scheme that is capable of providing the best outage performance for all-scale MH-TRCs. To generalize the outage performance analyse, the transmission pattern of the I-TTI MH-WNC scheme is converted to a binary tree model with corresponding transmission matrices. Theoretical studies on outage probability are carried out for the two well-known network coding schemes, i.e., ANC and compute-and-forward (CPF) network coding.

Gengkun Wang and Wei Xiang are with the Faculty of Health, Engineering and Sciences, University of Southern Queensland, Toowoomba, QLD 4350, AUSTRALIA (e-mail: {gengkun.wang, wei.xiang}@usq.edu.au)

Jinhong Yuan is with the School of Electrical Engineering and Telecommunications, University of New South Wales, Sydney, NSW 2052, AUSTRALIA (e-mail: j.yuan@unsw.edu.au).

The major contributions of this paper are multifold, which are summarized as follows:

- Proposal of a generalized transmission scheme of I-TTI MH-WNC for the L-node K-message MH-TRC;
- Derivation of closed-form expressions for the upper bound of the outage probability expressions of the MH-ANC and MH-CPF schemes;
- Evaluation of the relationships between the outage probability and the numbers of nodes, messages and TTIs; and
- Identification of the optimal MH-WNC scheme which can achieve the best outage performance and outperform Non-NC for all-scale MH-TRCs.

The remainder of the paper is organized as follows. In Section II, the system model of the generalized L-node K-message MH-TRC and transmission schemes are presented. Outage performance of MH-ANC is discussed in Section IV. We then analyse the outage probability of MH-CPF in Section V. The optimal MH-WNC scheme is presented in Section VI. Finally, concluding remarks are drawn in Section VII.

The notation used herein is given in Table I.

TABLE I
NOTATIONS.

Notation	Definition
P_l	Power per transmission for node N_l
$\mathbf{P}_S$	Single-access transmission power vector
$\mathbf{P}_M$	Multiple-access transmission power vector
S	Spectral efficiency
C	Network throughput
y_l^j	Received signal at node N_l in time slot j
x_l^j	Transmitted signal at node N_l in time slot j
$\mathbf{T}_{L,K}^I$	Transmission pattern matrix for I-TTI MH-WNC in a L-node K-message MH-TRC
$\mathbf{T}_{v_k}$	Transmission pattern matrix for message v_k
$\mathbf{N}_{v_k}$	Noise matrix for message v_k
$\tilde{\mathbf{N}}_{v_k}$	Noise power matrix for message v_k
$\mathbf{S}_{v_k}$	Signal matrix for message v_k
$\tilde{\mathbf{S}}_{v_k}$	Signal power matrix for message v_k
$\mathbb{S}_{v_k}$	Single-access matrix for message v_k
$\tilde{\mathbb{S}}_{v_k}$	Single-access power matrix for message v_k
$\mathbb{P}_{S,v_k}^{\text{out}}$	Single-access outage probability matrix for message v_k
$\mathbb{C}_{v_k}$	Multiple-access matrix for message v_k
$\tilde{\mathbb{C}}_{v_k}$	Multiple-access power matrix for message v_k
$\mathbb{P}_{C,v_k}^{\text{out}}$	Multiple-access outage probability matrix for message v_k

II. SYSTEM MODEL

Consider an MH-TRC with L nodes $\{N_l\}_{l=1}^L$, where user nodes N_1 and N_L exchange messages through intermediate relay nodes $\{N_l\}_{l=2}^{L-1}$. The message sequences to be transmitted by N_1 and N_L are denoted by $\mathbf{U} = \{u_k\}_{k=1}^K$ and $\mathbf{V} = \{v_k\}_{k=1}^K$, and the modulated signal sequences are defined as $\hat{\mathbf{U}} = \{\hat{u}_k\}_{k=1}^K$ and $\hat{\mathbf{V}} = \{\hat{v}_k\}_{k=1}^K$. It is assumed that only immediately neighboring nodes are within the transmission range in this network, and signals received from non-neighboring nodes are negligible due to signal attenuation.

In this paper, the overall system transmission power is assumed to be the same for both Non-NC and I-TTI MH-WNC schemes. Each node is assigned with transmission power P for one message exchange, i.e., each node is allocated with transmission power $2KP$ for K-message exchange. The greater the number of transmissions required at a node, the smaller the power per transmission will be. Denote by n_l the total number of transmissions at node N_l, the power per transmission for N_l is thus $P_l = 2KP/n_l$.

The channel coefficient between nodes N_l and N_{l+1} is denoted by $\{h_l\}_{l=1}^{L-1}$, which is considered quasi-static and reciprocal in bi-direction. For Rayleigh fading channels, $h_l \sim \mathcal{CN}(0, 2\alpha_l^2)$ is modeled as a zero mean, independent, circularly symmetric complex Gaussian random variable with variance α_l^2 per dimension. $\{\omega_l\}_{l=1}^L$ is the received noise at node N_l, which is a zero mean, independent, circularly symmetric, complex Gaussian random variable with the variance of σ^2. $\gamma_l' = |h_l|^2/\sigma^2$ is the signal-to-noise ratio (SNR) of hop l, which is exponentially distributed with parameter $1/\bar{\gamma}'_l$, with $\bar{\gamma}'_l = 2\alpha_l^2/\sigma^2$ indicating the average SNR of the channel.

A. Non-Network Coding

In this paper, we consider the multi-hop communication system to be symmetrical in terms of user message exchange. That is, the two end users exchange their messages one by one at an equal rate, and the exchange sequence is $\{(u_1, v_1), (u_2, v_2), ..., (u_K, v_K)\}$.

In conventional Non-NC schemes, intermediate terminals relay the signal from one hop to the next, as illustrated in Fig. 1(a). In non-regenerative systems, relays may amplify and forward the received signal from the previous node, whereas relays decode the signal and re-encode it prior to retransmission in regenerative systems. It takes $L-1$ time slots to forward one message from N_1 to N_L, and a total number of $\mathcal{T}_{\text{Non-NC}} = 2K(L-1)$ time slots are required to complete the message exchange.

Spectral efficiency for the MH-TRC is defined as the number of messages transmitted in a single time unit. Thus, the spectral efficiency of this conventional Non-NC scheme is $S_{\text{Non-NC}} = 1/L - 1$.

It should be noted that for the symmetrical message exchange pattern $\{(u_1, v_1), (u_2, v_2), ..., (u_K, v_K)\}$, the above conventional Non-NC scheme is the only scheme to avoid interference. However, if the symmetrical message exchange pattern is not required, e.g., the exchange sequence is $\{(u_1, u_2, ..., u_K), (v_1, v_2, ..., v_K)\}$, another asymmetrical Non-NC scheme can be applied, as shown in Fig. 1(b). Under this scheme, each node forwards the received signal to the next neighboring node every three time slots, and the transmissions do not overlap due to the two-hop intervals between them, as illustrated in Fig. 1(b) at time slot T_4. The total number of time slots required for this asymmetrical Non-NC scheme is $2(L-1)+6(K-1)$, and the spectral efficiency is $S_{\text{Asy-Non-NC}} = K/((L-1)+3(K-1))$. When the number of messages K is far larger than the number of nodes L, an upper limit can be obtained as $\hat{S}_{\text{Asy-Non-NC}} = \lim_{K>>L} \frac{K}{(L-1)+3(K-1)} = 1/3$.

The asymmetrical Non-NC scheme may improve the spectral efficiency. However, in the asymmetrical Non-NC scheme,

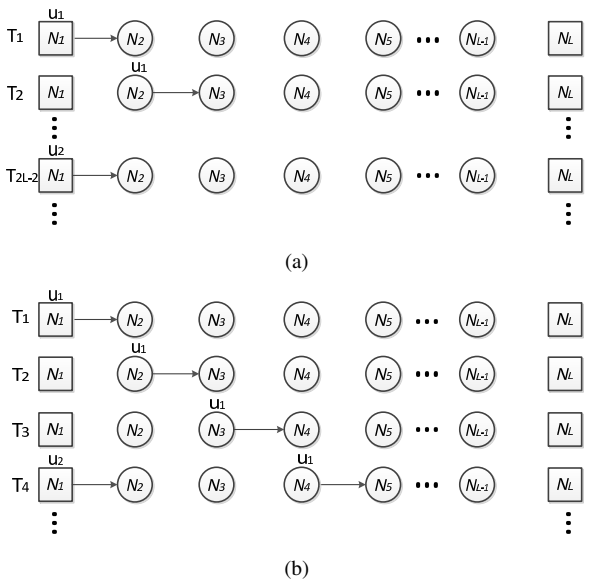

Fig. 1. (a) Conventional Non-NC scheme. Nodes N_1 and N_L take turns to transmit their messages until the end of the exchange process. Node N_L starts transmitting its message v_k after receiving the corresponding message u_k from its counterpart N_1, and so forth. The transmission pattern is $\{(u_1, v_1), (u_2, v_2), ..., (u_K, v_K)\}$; (b) Asymmetrical Non-NC scheme. User node N_1 transmits a new message every three time slots. For example, when node N_4 transmits message u_1 to N_5 in the fourth time slot, node N_1 sends u_2 to N_2 at the same time. Node N_L starts sending its messages after receiving all the K messages from node N_1, and follows the same transmission pattern as node N_1. The transmission pattern is $\{(u_1, u_2, ..., u_K), (v_1, v_2, ..., v_K)\}$.

one user node does not start sending its messages until it receives all the messages from its counterpart, which causes long delays in message exchange for this user node. Moreover, the resultant unequal message exchange leads to traffic imbalance and user unfairness issues between the two user nodes, in comparison with the symmetrical message exchange pattern. Furthermore, the asymmetrical exchange pattern is different from the symmetrical one, which is widely considered in the literature, e.g., the WNC scheme for the TWRC [8] [9] and the MH-WNC scheme for the MH-TRC [13] [14]. Therefore, the asymmetrical Non-NC scheme is not considered in this paper, and the Non-NC scheme we refer to in the following sections is the conventional Non-NC scheme illustrated by Fig. 1(a).

B. Generalized Wireless Network Coding Scheme

We now introduce WNC into the L-node K-message MH-TRC. Without loss of generality, we only consider that the number of nodes L is odd in this paper, while the case of even L can be easily extrapolated from the same procedure presented in this section.

Instead of sending their messages every two time slots as in the 2-TTI MH-WNC scheme, the two user nodes send one message every $I \geqslant 2$ time slots simultaneously, and the messages sent by N_1 and N_L in time slot $j \in \{1, I+1, ..., IK-1\}$ are $u_{(j-1)/I+1}$ and $v_{(j-1)/I+1}$, respectively. A total number of $IK-1$ time slots is required for the two user nodes to complete sending their message sequences.

Once the relay receives the messages from both neighboring nodes, it network-codes the received signal, and broadcasts the network-coded message to the neighboring nodes in the next transmission time slot. The received signal of the multiple-access phase at relay node N_l in time slot j is given by

$$y_l^j = \sqrt{P_{l-1}} h_{l-1} x_{l-1}^j + \sqrt{P_{l+1}} h_l x_{l+1}^j + w_l^j, \quad (1)$$

where x_l^j is the transmitted signal by relay node N_l in time slot j, and w_l^j denotes the received noise at node N_l in time slot j. For non-regenerative relaying strategies, the transmitted signal x_l^j is simply a scaled version of the received signal from the previous time slot y_l^{j-1}. For regenerative relaying strategies, the transmitted signal x_l^j is a network-coded codeword decoded from y_l^{j-1} (an XORed message with "standard" PNC, or a linear combination with CPF).

After time slot $L-1$, the two user nodes N_1 and N_L will receive the signal containing the messages from the counterpart every I time slots. Knowing its own messages, the user nodes can extract the required messages. For the non-generative MH-TRC, the user nodes cancel their own signals and decode required messages. On the other hand, the user nodes decode the linear combination of outgoing and incoming messages, and solve the linear equations for the required messages in the regenerative MH-TRC.

Let $\mathbb{R}$, $\mathbb{T}$ and $\ominus$ denote the receiving, sending and silent modes of the nodes, respectively. Denote by $\mathbb{S}_l^j$ the operation mode for node N_l in time slot j. The transmission modes for each node in different time slots with MH-WNC can be summarized as

- For user nodes N_1 and N_L:
  $\mathbb{S}_1^j = \mathbb{S}_L^j = \mathbb{T}$, $j \in \{1, I+1, 2I+1, ..., (K-1)I+1\}$.
  $\mathbb{S}_1^j = \mathbb{S}_L^j = \mathbb{R}$, $j \in \{L-1, L-1+I, L-1+2I, ..., L-1+I(K-1)\}$.
  $\mathbb{S}_1^j = \mathbb{S}_L^j = \ominus$, other.
- For relay nodes $\{N_l\}_{l=2}^{L-1}$:
  $\mathbb{S}_l^j = \mathbb{T}$, $j \in \{L-l+1, L-l+I+1, L-l+2I+1, ..., L-l+(K-1)I+1\} \cup \{l+1, l+I+1, l+2I+1, ..., l+(K-1)I+1\}$.
  $\mathbb{S}_l^j = \mathbb{R}$, if $\mathbb{S}_{l-1}^j = \mathbb{T} \cup \mathbb{S}_{l+1}^j = \mathbb{T}$.
  $\mathbb{S}_l^j = \ominus$, other.

Let -1 represent the single-access mode, 1 represent the transmission mode, 0 represent the silent mode, and -2 represent the multiple-access mode. The transmission pattern can be represented by a $\mathcal{T}$ (the number of time slots) by L (the number of nodes) transmission matrix $\mathbf{T}_{L,K}^I$. For example, the transmission matrix of 2-TTI MH-WNC for the 5-node 2-message MH-TRC can be expressed as

$$\mathbf{T}_{5,2}^2 = \begin{bmatrix} 1 & -1 & 0 & -1 & 1 \\ 0 & 1 & -2 & 1 & 0 \\ 1 & -2 & 1 & -2 & 1 \\ -1 & 1 & -2 & 1 & -1 \\ 0 & -1 & 1 & -1 & 0 \\ -1 & 1 & 0 & 1 & -1 \end{bmatrix}, \quad (2)$$

where each element represents the mode of node N_i at time

slot j. For example, the first row $[1, -1, 0, , -1, 1]$ represents that N_1 is transmitting a message to N_2, N_5 is transmitting a message to N_4, and N_3 is in the silent mode. In this paper, we devise a grid chart to display the transmission pattern via the matrix, e.g., the grid chart of 2-TTI MH-WNC for the 11-node 3-message MH-TRC is illustrated in Fig. 2.

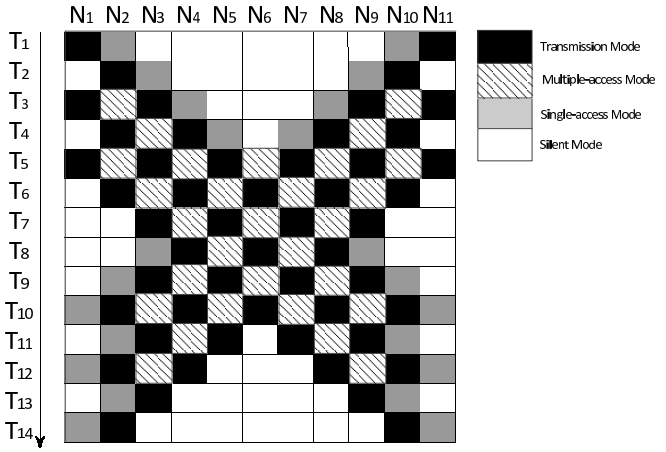

Fig. 2. Grid chart of 2-TTI MH-WNC for the 11-node 3-message MH-TRC. The horizontal grids represent the L nodes, and the vertical grids represent the $\mathcal{T}$ time slots. The colour of each grid indicates the operation mode of the corresponding node in a specific time slot.

With I-TTI MH-WNC, the total number of time slots for exchanging the two message sequences is $\mathcal{T}_{\text{MH-WNC}} = L - 1 + I(K-1)$. The spectral efficiency is $S_{\text{MH-WNC}} = 2K/(L-1+I(K-1))$. When the number of messages is far larger than the number of nodes, an upper limit of $S_{\text{MH-WNC}}$ can be obtained as $\hat{S}_{\text{MH-WNC}} = \lim_{K>>L-1-I} \frac{2K}{L-1+I(K-1)} = 2/I$. In comparison with Non-NC, the generalized MH-WNC scheme markedly improves the spectral efficiency.

III. Outage Performance of Multi-Hop Analog Network Coding

In this section, we will analyse the performance of MH-ANC for the non-regenerative MH-TRC, including the average received SNR and outage probability.

There is a large body of literature on the performance analyse of the traditional amplify-and-forward (AF) scheme in multi-hop relay networks, which is related to the work presented in this section. Hasna *et al.* [20] derived the analytical expressions of the harmonic mean and cumulative density function of the average received SNR for two-hop relay networks, which can be applied to outage performance and average bit-error-rate (BER) analyse. Then, they generalized the outage probability of the multi-hop relay network over Nakagami fading channels in [21]. In [11], the authors analysed the performance of ANC in a single relay TWRC. Closed-form expressions of the average received SNR, outage probability, sum-bit-error-rate and maximum sum-rate for the traditional three time slot network coding, and ANC schemes were derived. In this paper, this previous work on the non-regenerative MH-TRC will be used as a benchmark in the outage performance analyse.

The AF relaying strategy is applied at each relay in MH-ANC, and the transmitted signal of relay node N_l in time slot j is a scaled version of the received signal in the previous time slot $x_l^j = G_l y_l^{j-1}$, where G_l represents the gain at relay nodes N_l, which is set to

$$G_l^1 = \sqrt{\frac{1}{P_{l-1}|h_{l-1}|^2 + \sigma^2}}, \qquad N_{l-1} \overset{a}{\rightarrow} N_l, \tag{3}$$

$$G_l^2 = \sqrt{\frac{1}{P_l|h_l|^2 + \sigma^2}}, \qquad N_l \overset{a}{\leftarrow} N_{l+1}, \tag{4}$$

$$G_l^3 = \sqrt{\frac{1}{P_{l-1}|h_{l-1}|^2 + P_{l+1}|h_l|^2 + \sigma^2}}, N_{l-1} \overset{a}{\rightarrow} N_l \overset{a'}{\leftarrow} N_{l+1} \tag{5}$$

where $N_{l-1} \overset{a}{\rightarrow} N_l$ denotes that N_{l-1} transmits message a to N_l. After time slot $L-1$, the two user nodes will receive the signal containing the messages from the counterpart user node every I time slots. Knowing their own messages, user nodes can cancel these signals in the analog field and decode the required messages.

A. Received SNR

For the MH-ANC scheme, the message is amplified and forwarded bi-directionally at the relay nodes throughout the exchange process. Hence, the received signal at N_1 consists of the outgoing messages, incoming messages, and the received noise at intermediate relays. For the L-node MH-TRC with a I-TTI MH-ANC scheme, the received signal at N_1 can be expressed as (6), (7) and (8), where $\psi_{i,l}^j$, $\varphi_{i,l}^j$ and ϕ_l^j are the polynomials of P_l, G_l and h_l for term $\hat{u}_i$, $\hat{v}_i$ and ω_l^j at time slot j, respectively. In this paper, it is assumed that the two user nodes have the knowledge of the channel state information (CSI) of the channels, via pilot transmission during which the CSI can be estimated and passed to the user nodes. Note that N_1 has the knowledge of its own transmitted messages $\{u_1, u_2, ..., u_K\}$, it can cancel the terms of $\hat{u}_i$ and extract $\hat{v}_1$ at time slot $L-1$, as shown in (6). At time slot $L-1+I$, N_1 can extract $\hat{v}_2$ with the knowledge of its own transmitted messages and the message $\hat{v}_1$ extracted at time slot $L-1$, as shown in (7). The operation continues to decode all the incoming messages every I time slots.

Hence, the resulting signal of message v_k after canceling the outgoing and previously extracted messages can be derived from (8) as

$$y^*_{\text{MH-ANC},v_k} = \sum_{l\in\{1,L\}, j\in\{1,\mathcal{T}_{\text{MH-ANC},v_k}\}} \left(\varphi_{k,l}^j \hat{v}_k + \phi_l^j \omega_l^j\right). \tag{9}$$

The received SNR of message v_k can be obtained as

$$\gamma_{\text{MH-ANC},v_k} = \frac{\sum_{l\in\{1,L\}, j\in\{1,\mathcal{T}_{\text{MH-ANC},v_k}\}} |\varphi_{k,l}^j|^2}{\sum_{l\in\{1,L\}, j\in\{1,\mathcal{T}_{\text{MH-ANC},v_k}\}} |\phi_l^j|^2 \sigma^2}. \tag{10}$$

where the signal power $|v_k|^2 = 1$ under the assumption that

$$y_{\text{MH-ANC},v_1} = \sum_{i=1}^{\lfloor \frac{L-1}{I} \rfloor} \sum_{l\in\{1,L\},j\in\{1,L-1\}} \psi_{i,l}^{j}\hat{u}_i + \sum_{l\in\{1,L\},j\in\{1,L-1\}} \varphi_{1,l}^{j}\hat{v}_1 + \sum_{l\in\{1,L\},j\in\{1,L-1\}} \phi_l^j \omega_l^j, \tag{6}$$

$$\begin{aligned} y_{\text{MH-ANC},v_2} = & \sum_{i=1}^{\lfloor \frac{L-1+I}{I} \rfloor} \sum_{l\in\{1,L\},j\in\{1,L-1+I\}} \psi_{i,l}^{j}\hat{u}_i + \sum_{l\in\{1,L\},j\in\{1,L-1+I\}} \varphi_{1,l}^{j}\hat{v}_1 + \sum_{l\in\{1,L\},j\in\{1,L-1+I\}} \varphi_{2,l}^{j}\hat{v}_2 \\ & + \sum_{l\in\{1,L\},j\in\{1,L-1+I\}} \phi_l^j \omega_l^j, \end{aligned} \tag{7}$$

$$\cdots\cdots$$

$$\begin{aligned} y_{\text{MH-ANC},v_k} = & \sum_{i=1}^{\lfloor \frac{\mathcal{T}_{\text{MH-ANC},v_k}}{I} \rfloor} \sum_{l\in\{1,L\},j\in\{1,\mathcal{T}_{\text{MH-ANC},v_k}\}} \psi_{i,l}^{j}\hat{u}_i + \sum_{i=1}^{k-1} \sum_{l\in\{1,L\},j\in\{1,\mathcal{T}_{\text{MH-ANC},v_k}\}} \varphi_{i,l}^{j}\hat{v}_i \\ & + \sum_{l\in\{1,L\},j\in\{1,\mathcal{T}_{\text{MH-ANC},v_k}\}} \varphi_{k,l}^{j}\hat{v}_k + \sum_{l\in\{1,L\},j\in\{1,\mathcal{T}_{\text{MH-ANC},v_k}\}} \phi_l^j \omega_l^j, \end{aligned} \tag{8}$$

binary phase-shift keying (BPSK) modulation is used at all the nodes.

Two recursive approaches were proposed in [16] to derive the analytical polynomials φ_l^j and ϕ_l^j for the 2-TTI MH-ANC. However, it is difficult to devise an universal recursive approach for the generalized I-TTI MH-ANC scheme, because the transmission patterns are different for the MH-ANC schemes with different TTIs. Therefore, by utilizing the transmission pattern matrix of each message, we design a numerical algorithm to compute φ_l^j and ϕ_l^j, thus the received SNR for each message.

For the purpose of theoretical analysis and following other work in the literature [22] [23], we assume that all the channels have the same amplitude, i.e., $|h_l|^2 = |h|^2$. It is noted that this assumption is only made for analytical convenience. i.e., the derivation of outage performance and the comparison with the conventional Non-NC schemes. The implementation of the protocol in practical communications networks will not be constrained by this assumption due to the availability of some practical mechanism such as pilot transmission to acquire the CSI of the channels before message exchange.

Denote by $\{W_l\}_{l=1}^{L}$ the weight as the power of amplification factor at each node, three different weights corresponding the amplification factors given by (3), (4) and (5) at node N_l can be obtained as

$$W_l^1 = \frac{P_l|h|^2}{P_{l-1}|h|^2+\sigma^2}, \qquad N_{l-1} \xrightarrow{a} N_l, \tag{11}$$

$$W_l^2 = \frac{P_l|h|^2}{P_{l+1}|h|^2+\sigma^2}, \qquad N_l \xleftarrow{a} N_{l+1}, \tag{12}$$

$$W_l^3 = \frac{P_l|h|^2}{(P_{l-1}+P_{l+1})|h|^2+\sigma^2}, \quad N_{l-1} \xrightarrow{a} N_l \xleftarrow{a'} N_{l+1}. \tag{13}$$

Since only some transmission events affect the noise propagation, the transmission matrix for each message can be further converted into a characteristic matrix that only contains the effective transmission events. By applying different weights into these transmission events, the noise power matrix for message v_k can be computed as

$$\tilde{\mathbf{N}}_{v_k} = \sum_{i=1}^{3} \left(\mathbf{N}_{v_k}^{i} \circ \mathbf{W}^{i} \right), \tag{14}$$

where $\mathbf{N}_{v_k}^{i}$ is the noise matrix containing only the transmission event with weight W_l^i, and $A \circ B = [a_{ij}]_{m\times n} \circ [b_j]_{n\times 1} = [a_{ij} * b_j]_{m\times n}$.

The propagation of the noise power is simply the traversal of the weights at each non-zero node in the noise power matrix. The following post-order traversal approach is proposed to obtain the noise power.

Algorithm: Post-order traversal algorithm for the noise power matrix $\mathbf{N}_{v_k}$

Input: Noise power matrix $\mathbf{N}_{v_k}$.

Output: Noise power $\mathcal{N}_{v_k}$.

1.$\mathbf{Nn}$ =ZEROS($\mathcal{T}_i \times L$)
2.**for** i=1 to $\mathcal{T}_i$ **do**
3. **for** j=1 to L **do**
4. **if** $\mathbf{C}_{v_i}(i,j) = 0$ **then**
5. $\mathbf{Nn}(i,j) \leftarrow 0$
6. **end if**
7. **if** $\mathbf{C}_{v_i}(i,j) \neq 0$ **then**
8. $\mathbf{Nn}(i,j) \leftarrow (\mathbf{Nn}(i+1,j-1) + \mathbf{Nn}(i+1,j+1)) \times \mathbf{C}_{v_i}(i,j)$
9. **end if**
10. **end for**
11.**end for**
12.**return** $\mathcal{N}_{v_k} \leftarrow SUM(\mathbf{Nn}) + 1$

Hence, the noise power then can be calculated by traversing

the noise power matrix as

$$\mathcal{N}_{\text{MH-ANC},v_k} = \text{Trv}\left(\tilde{\mathbf{N}}_{v_k}\right)\sigma^2, \tag{15}$$

where $\text{Trv}(\cdot)$ stands for the post-order traversal algorithm.

Similarly, the signal power matrix can be obtained as

$$\tilde{\mathbf{S}}_{v_k} = \sum_{i=1}^{4}\left(\mathbf{S}_{v_k}^i \circ \mathbf{W}^i\right), \tag{16}$$

where $\mathbf{S}_{v_k}^i$ is the signal matrix containing only the transmission event with weight W_l^i, and $\mathbf{W}^4 = \{W_l^4 = P_l|h|^2\}_{l=1}^L$.

The signal power is simply the product of all non-zero elements in the signal power matrix, given by

$$\mathcal{S}_{\text{MH-ANC},v_k} = \text{Prod}_{\text{nz}}\left(\tilde{\mathbf{S}}_{v_k}\right), \tag{17}$$

where $\text{Prod}_{\text{nz}}(\cdot)$ indicates the product of all non-zero elements of the matrix.

Then, the received SNR of message v_k can be calculated by dividing the signal power in (17) by the noise power in (15) as

$$\gamma_{\text{MH-ANC},v_k} = \frac{\mathcal{S}_{\text{MH-ANC},v_k}}{\mathcal{N}_{\text{MH-ANC},v_k}} = \frac{\text{Prod}_{\text{nz}}\left(\tilde{\mathbf{S}}_{v_k}\right)}{\text{Trv}\left(\tilde{\mathbf{N}}_{v_k}\right)\sigma^2}. \tag{18}$$

B. Upper Bound of the Received SNR

In high SNR regions, the three weights given by (11), (12) and (13) can be upper-bounded as

$$\hat{W}_l^1 = \frac{P_l|h|^2}{P_{l-1}|h|^2+\sigma^2} = \left.\frac{\frac{2KP}{n_l}\gamma'}{\frac{2KP}{n_{l-1}}\gamma'+1}\right|_{\gamma'\to\infty} = \frac{n_{l-1}}{n_l}, \tag{19}$$

$$\hat{W}_l^2 = \frac{n_{l+1}}{n_l}, \tag{20}$$

$$\hat{W}_l^3 = \frac{n_{l-1}n_{l+1}}{n_l(n_{l-1}+n_{l+1})}, \tag{21}$$

where n_l is the total number of transmissions of node N_l, which is constant only determined by L, K, I.

Therefore, it can be deduced that, in high SNR regions, the noise power given by (15) is a scaled version of σ^2, i.e., $f_k^N\sigma^2$, and the signal power given by (17) is also a scaled version of $W_l^4 = P_l|h|^2$, i.e., $f_k^S P_l|h|^2 = \frac{f_k^S 2KP|h|^2}{n_l}$, the received SNR of v_k given by (18) can be simplified as

$$\hat{\gamma}_{\text{MH-ANC},v_k} = \frac{\frac{f_k^S 2KP|h|^2}{n_l}}{f_k^N\sigma^2} = f_k P\gamma', \tag{22}$$

where $\gamma' = \frac{|h|^2}{\sigma^2}$ and $f_k = \frac{f_k^S 2K}{f_k^N n_l}$.

The upper bound of the average received SNR for the L-node K-message MH-TRC can be given by

$$\hat{\gamma}_{\text{MH-ANC}} = \frac{1}{K}\sum_{k=1}^{K}\hat{\gamma}_{\text{MH-ANC},v_k} = \frac{1}{K}\sum_{k=1}^{K} P f_k\gamma' = F_K P\gamma' \tag{23}$$

where $F_K = \frac{1}{K}\sum_{k=1}^{K} f_k$.

C. Outage Probability

The maximum mutual information for I-TTI MH-ANC can be shown as

$$I_{\text{MH-ANC}} = C_{\text{MH-ANC}}\log(1+\gamma_{\text{MH-ANC}}). \tag{24}$$

Given a target rate R, the upper-bound outage probability in high SNR regions can be derived as

$$\begin{aligned}\hat{p}_{\text{MH-ANC}}^{\text{out}}(R) &= \Pr\left[C_{\text{MH-ANC}}\log\left(1+F_K P\gamma'\right) < R\right] \\ &= F_{\gamma'}\left(\frac{2^{\frac{1}{C_{\text{MH-ANC}}}R}-1}{F_K P}\right) \\ &= 1-\exp\left(-\underbrace{\frac{2^{\frac{1}{C_{\text{MH-ANC}}}R}-1}{F_K P\bar{\gamma}'}}_{\mathcal{A}}\right),\end{aligned} \tag{25}$$

where $F_{\gamma'}(x)$ is the cumulative density function (CDF) of γ'.

The outage probability given in (25) can be computed analytically, because that both $C_{\text{MH-ANC}}$ and F_K are constants and can be readily obtained by the algorithms presented in this section. More specifically, the received SNR derivation example for message v_1 in the 5-node 2-message MH-TRC with 2-TTI MH-ANC is presented in Appendix A to explain the derivation.

IV. Outage Performance of Multi-Hop Compute-and-Forward Network Coding

Compute-and-forward network coding strategy was proposed recently to realize reliable PNC [24], where the relays compute and forward linear combinations of user messages to destinations. It is noted that for BPSK, when the two integer coefficients are set to 1 in a two-user multiple-access channel, the linear combination is equivalent to the modular-2 addition in "standard" PNC [8], which is also implied in [25, Remark 4] and [26, Section II-B].

In MH-CPF, relay nodes compute linear combinations of messages from neighboring nodes and broadcast to them in next transmitting time slots. The received signal given by (1) can be rewritten as

$$y_l^j = \mathbf{D}_l\left[x_{l-1}^j\ x_{l+1}^j\right]^T + w_l^j, \tag{26}$$

where $\mathbf{D}_l = [\sqrt{P_{l-1}}h_{l-1}\ \sqrt{P_{l+1}}h_l]$, x_{l-1}^j and x_{l+1}^j are the transmitted signals from neighboring relay nodes N_{l-1} and N_{l+1}, which are the decoded linear combinations at the relay nodes in the previous time slot.

After receiving the interference signal, the relay node selects a complex integer coefficient vector $\mathbf{a}_l^j \in \{\mathbb{Z}+\mathbb{Z}i\}^2$ and decodes the following linear combination

$$x_l^j = \mathbf{a}_l^j\left[x_{l-1}^{j-1}\ x_{l+1}^{j-1}\right]^T. \tag{27}$$

After time slot $L-1$, the two user nodes N_1 and N_L will receive linear combinations of the outgoing and incoming messages every I time slot. In order to solve the linear combination, the user nodes have to know the choices of $\mathbf{a}_l^j$ at each relay node, which can be forwarded via, e.g., the package header during the transmission. Knowing its own messages

and the complex integer coefficient vector $\mathbf{a}_l^j$, the user nodes are able to solve the linear combination for their required messages.

In this paper, all the channels are assumed to be quasi-static, implying that the instantaneous channel state information of h_l remains unchanged during the entire exchange process. Therefore, the maximized computation rate $R_{\text{COMP},l}(\mathbf{h}_l, \mathbf{a}_l^j)$ for decoding the linear combination x_l^j at relay N_l disregards the time slot j, and remains unchanged during the entire exchange process. Thus, the computation rate at relay N_l can be given by [25]

$$R_{\text{COMP},l}(\mathbf{D}_l, \hat{\mathbf{a}}_l) = \log^+\left(||\hat{\mathbf{a}}_l||^2 - \frac{|\hat{\mathbf{a}}_l \mathbf{D}_l^\dagger|^2}{n_0 + ||\mathbf{D}_l||^2}\right)^{-1}, \quad (28)$$

where $\log^+(x) \triangleq \max(\log(x), 0)$ and $\hat{\mathbf{a}}_l = [\vec{a}_l, \overleftarrow{a}_l]$. $\vec{a}_l$ and $\overleftarrow{a}_l$ are two complex integer coefficients corresponding to the two messages x_{l-1}^{j-1} and x_{l+1}^{j-1} in linear combination x_l^j, respectively. According to Theorem 1 in [27] and Proposition 1 in [28], the above maximization problem amounts to the following shortest vector problem (SVP),

$$\hat{\mathbf{a}}_l = \arg\min_{\mathbf{a}_l \neq 0} ||\mathbf{a}_l \mathbf{L}||, \quad (29)$$

where $\mathbf{L}$ is the Cholesky decomposition matrix of $\mathbf{I} - \frac{\mathbf{D}_l^\dagger \mathbf{D}_l}{n_0 + ||\mathbf{D}_l||^2}$, and $\mathbf{I}$ is an $L \times L$ identity matrix.

For the above special two-dimensional case in Rayleigh fading channels, the complex lattice reduction algorithm proposed in [29] can be applied to solve the above SVP and obtain the maximized computation rate efficiently.

Each message follows a different transmission path, and failing to decode one message will affect the decoding of the following messages. The outage probabilities of later messages are poorer than those of early messages.

Given a target rate R, the average outage probability per message is defined as

$$p^{\text{out}}(R) = \frac{1}{K} \sum_{k=1}^{K} p_{v_k}^{\text{out}}(R), \quad (30)$$

where $p_{v_k}^{\text{out}}(R)$ is the outage probability of message v_k, which is identical to the outage probability of message u_k due to the symmetrical property of the two-way transmission. The outage event of message v_k occurs when any of the transmissions that affect the transmission of message v_k are in outage.

In order to determine the outage probability for each message, we first define $f_{S,l}^j$ and $f_{M,l}^j$ as the single-access and multiple-access transmission events at node N_l in time slot j,

$$f_{S,l}^j \triangleq \left\{N_{l-1} \xrightarrow{a} N_l\right\} \cup \left\{N_l \xleftarrow{a} N_{l+1}\right\},$$
$$f_{M,l}^j \triangleq \left\{N_{l-1} \xrightarrow{a} N_l \xleftarrow{a'} N_{l+1}\right\},$$
$$\forall l \in \{1, 2, ..., L\}, \forall j \in \{1, 2, 3, ...\},$$

and $\mathcal{F}_{v_k}$ as the set of all the transmission events that affect the transmission of message v_k,

$$\mathcal{F}_{v_k} \triangleq \left\{\{f_{S,l}^j, f_{M,l}^j\}_{l \in \{1,2,...,L\}}^{j \in \{1,2,...,\mathcal{T}_k\}}\right\}, \quad \forall k \in \{1, 2, ..., K\},$$

Thus, the outage event of message v_k occurs when any single access transmission event $f_{S,l}^j$ or multiple-access transmission evens $f_{M,l}^j$ in set $\mathcal{F}_{v_k}$ is in outage, given by

$$p_{v_k}^{\text{out}}(R) = 1 - \underbrace{\prod_{f_{S,l}^j \in \mathcal{F}_{v_k}} \left(1 - p_{f_{S,l}^j}^{\text{out}}(R_{\text{MH-CPF}})\right)}_{\mathcal{B}_k} \underbrace{\prod_{f_{M,l}^j \in \mathcal{F}_{v_k}} \left(1 - p_{f_{M,l}^j}^{\text{out}}(R_{\text{MH-CPF}})\right)}_{\mathcal{C}_k}, \quad (31)$$

where $R_{\text{MH-CPF}}$ is the message target rate for each transmission, given by $R_{\text{MH-CPF}} = R/C_{\text{MH-CPF}}$.

A. Single-Access Transmission Event

The single transmission event matrix $\mathbb{S}_{v_k}$ can be extracted from the transmission pattern matrix of message v_k, by setting to 1 the corresponding elements (whose left or right neighboring element in the transmission matrix $\mathbf{T}_{v_k}$ is -1). For example, the single access transmission matrix of message v_1 for the 5-node 2-message MH-TRC with 2-TTI MH-CPF scheme can be obtained as

$$\mathbb{S}_{v_1} = \begin{bmatrix} 1 & 0 & 0 & 0 & 1 \\ 0 & 0 & 0 & 0 & 0 \\ 0 & 0 & 1 & 0 & 0 \\ 0 & 1 & 0 & 0 & 0 \end{bmatrix}. \quad (32)$$

It is assumed that all the channel coefficients are identical. Therefore, for the single access transmission, the outage probability is only determined by the transmission power at each transmission. The transmission power vector of the L-node MH-TRC can be written as $\mathbf{P}_S = [P_1 \quad P_2 \quad P_3 \cdots P_l \cdots \quad P_L]$, where P_l is the power per transmission of node N_l.

The single access transmission power matrix (each element denotes the transmission power of the corresponding transmission event) can be obtained as

$$\tilde{\mathbb{S}}_{v_k} = \mathbb{S}_{v_k} \circ \mathbf{P}_S^T. \quad (33)$$

Given a target rate R, the single access transmission outage probability matrix of message v_k (the elements are the outage probability of each single access transmission) can then be written as

$$\mathbb{P}_{S,v_k}^{\text{out}} = J_{\mathcal{T}_{v_k}}^L - \exp\left(-\frac{(2^{\frac{R}{C_{\text{MH-CPF}}}} - 1)}{\bar{\gamma}} . * \tilde{\mathbb{S}}_{v_k}\right), \quad (34)$$

where $J_{\mathcal{T}_{v_k}}^L$ is a $\mathcal{T}_{v_k}$ by L matrix of ones, and $(.*)$ represents element-wise multiplication operation.

The element in $\mathbb{P}_{S,v_k}^{\text{out}}$ is the outage probability of all the single access transmission events that affect the transmission of message v_k. Therefore, term $\mathcal{B}_k$ in (31) can be obtained as

$$\mathcal{B}_k = \text{Prod}\left(J_{\mathcal{T}_{v_k},L} - \mathbb{P}_{S,v_k}^{\text{out}}\right), \quad (35)$$

where Prod$(\cdot)$ represents the product of all the elements in the matrix.

B. Multiple-Access Transmission Event

It is assumed that all the channels have the same amplitude, i.e., $|h_l|^2 = |h|^2$. Therefore, the computation rate is determined only by the transmission powers of the neighboring nodes and the integer coefficient vector $\hat{\mathbf{a}}_l$, as can be seen from (28). Hence, the power vector for the multiple-access transmission can be written as $\mathbf{P}_M = [P_{M,1} \quad P_{M,2} \quad P_{M,3} \cdots P_{M,l} \cdots P_{M,L}]$, where each element $P_{M,l} = (P_{l-1}, P_1)$ contains the transmission powers of the two neighboring nodes of N_l, and $P_{M,1} = P_{M,L} = (0, 0)$.

The CPF matrix $\mathbb{C}_{v_k}$ can be extracted from the transmission matrix of message v_k, by setting the corresponding elements whose value in the transmission matrix $\mathbf{T}_{v_k}$ is -2 to 1. For example, the CPF matrix of message v_1 for the 5-node 2-message MH-TRC with the 2-TTI MH-CPF scheme can be obtained as

$$\mathbb{C}_{v_1} = \begin{bmatrix} 0 & 0 & 0 & 0 & 0 \\ 0 & 0 & 1 & 0 & 0 \\ 0 & 0 & 0 & 0 & 0 \\ 0 & 0 & 0 & 0 & 0 \end{bmatrix}. \tag{36}$$

Multiplying the CPF matrix $\mathbb{C}_{v_k}$ by the power vector $\mathbf{P}_M$, the CPF power matrix can be obtained as

$$\tilde{\mathbb{C}}_{v_k} = \mathbb{C}_{v_k} \circ \mathbf{P}_M^T. \tag{37}$$

For a given target rate R, the CPF outage probability matrix whose elements are the outage probability of each CPF process, can then be given by

$$\mathbb{P}^{\text{out}}_{M,v_k} = \text{CPF}\left(\tilde{\mathbb{C}}_{v_k}\right), \tag{38}$$

where CPF$(\cdot)$ represents the algorithm for calculating the outage probability of each non-zero element. Due to page limitation, we are unable to include this algorithm here, while interested readers can refer to our previous work in [17].

The element in $\mathbb{P}^{\text{out}}_{M,v_k}$ is the outage probability for all the multiple-access transmission events that affect the transmission of message v_k. Therefore, term $\mathcal{C}$ in (31) can then be obtained as

$$\mathcal{C}_k = \text{Prod}\left(J_{\mathcal{T}_{v_k},L} - \mathbb{P}^{\text{out}}_{M,v_k}\right). \tag{39}$$

Substituting (31) to (30), the outage probability for I-TTI MH-CPF can be obtained as

$$\begin{aligned} & p^{\text{out}}_{\text{MH-CPF}}(R) \\ &= \frac{1}{K}\sum_{k=1}^{K}(1 - \mathcal{B}_k \cdot \mathcal{C}_k) \\ &= 1 - \frac{1}{K}\sum_{k=1}^{K}\left[\text{Prod}\left(J^L_{\mathcal{T}_{v_k}} - \mathbb{P}^{\text{out}}_{S,v_k}\right) \cdot \text{Prod}\left(J^L_{\mathcal{T}_{v_k}} - \mathbb{P}^{\text{out}}_{M,v_k}\right)\right]. \end{aligned} \tag{40}$$

It should be noted that, the two outage matrices $\mathbb{P}^{\text{out}}_{S,v_k}$ and $\mathbb{P}^{\text{out}}_{S,v_k}$ can be readily obtained through the proposed algorithms. Moreover, the two matrices are only determined by L, K, I. Therefore, the outage probability of the I-TTI MH-CPF for the L-node K-message MH-TRC given by (40) can be computed analytically.

V. Numerical Results

In this section, we will investigate the relationships between the outage probability and the numbers of nodes, messages, and TTIs of I-TTI MH-WNC, so as to determine the optimal MH-WNC scheme for all-scale MH-TRCs. The transmission power per message P is normalized to 1 in the following numerical results.

The spectral efficiency of I-TTI MH-WNC is determined by the number of nodes (L), the number of messages (K), and the number of TTIs (I). Denote by $f_{sp}(L, K, I)$ the spectral efficiency function of I-TTI MH-WNC, we have

- $f_{sp}(L, K, I_1) < f_{sp}(L, K, I_2), \quad \forall I_1 > I_2,$ (41)
- $f_{sp}(L, K_1, I) > f_{sp}(L, K_2, I), \quad \forall K_1 > K_2,$ (42)

  $f_{sp}(L, K, I) \approx \frac{2}{I}, \quad \forall K \gg L - 1 - I,$ (43)
- $f_{sp}(L_1, K, I) < f_{sp}(L_2, K, I), \quad \forall L_1 > L_2.$ (44)

A. Multi-Hop Analog Network Coding

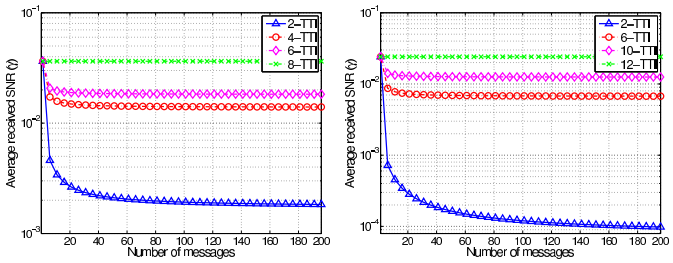

(a) (b)

Fig. 3. Average received SNR versus the number of messages for the MH-TRCs of different scales. (a) 9-node MH-TRC; and (b) 13-node MH-TRC.

Fig. 3 plots the upper bound of the average received SNR (as given by (23)) for I-TTI MH-ANC versus the number of messages, where the average received SNR is measured by γ' (the average SNR per hop). As can be seen from the figures, the average received SNR decreases with the number of messages when $I < L-1$, and remains unchanged regardless of the number of messages when $I = L - 1$. Moreover, the average received SNR becomes steady when the number of messages is large. The figure also demonstrates that the average received SNR of the MH-ANC scheme with larger TTIs is larger than the MH-ANC scheme with a smaller number of TTIs.

Fig. 4 shows the upper bound of the average received SNR versus the number of nodes for the MH-ANC scheme with a various numbers of TTIs. It can be found that the average received SNR decreases with the number of nodes. Furthermore, when the number of TTIs is far larger than that of the hops, the transmission of later messages is not affected by the transmission of early messages. Therefore, it can be seen from the figure that the average received SNR remains almost unchanged regardless of the number of messages.

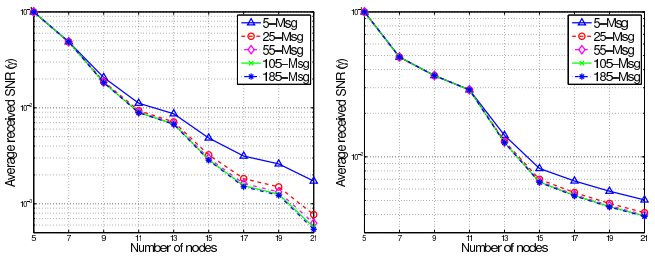

(a) (b)

Fig. 4. Average received SNR versus the number of nodes for the MH-ANC scheme with various numbers of TTIs. (a) 6-TTI MH-ANC; and (b) 10-TTI MH-ANC.

Denote by $f_s(L,K,I)$ the average received SNR of the L-node K-message MH-TRC with I-TTI MH-ANC, we have

- $f_s(L,K,I_1) > f_s(L,K,I_2), \forall I_1, I_2 < L-1, I_1 > I_2$ (45)
  $f_s(L,K,I_1) \equiv f_s(L,K,I_2), \quad \forall I_1, I_2 \geqslant L-1,$ (46)
- $f_s(L,K_1,I) < f_s(L,K_2,I), \forall K_1 > K_2,,$ (47)
  $f_s(L,K_1,I) \equiv f_s(L,K_2,I), \quad \forall K_1, K_2 \gg L-1-I,$ (48)
- $f_s(L_1,K,I) < f_s(L_2,K,I), \forall L_1 > L_2.$ (49)

It can be inferred from (41), (42), (45) and (47) that the monotonic characteristics of the spectral efficiency with K, I are actually opposite to that of the average SNR. Therefore, the numerator and denominator of term $\mathcal{A}$ in (25) have the same monotonous characteristics. It is difficult to determine the monotonic characteristic of the outage probability with K, I only by Equation (25) intuitively.

Lemma 1: Denote by $f^o_{\text{MH-ANC}}(L,K,I)$ the outage probability of the L-node K-message MH-TRC with I-TTI MH-ANC, we have

$$f^o_{\text{MH-ANC}}(L,K,I_1) < f^o_{\text{MH-ANC}}(L,K,I_2), \quad \forall I_1 > I_2, I_1, I_2 \geqslant L-1,$$

Proof: The outage probability of the L-node K-message MH-TRC with I-TTI MH-ANC can be written as

$$f^o_{\text{MH-ANC}}(L,K,I) = 1 - \exp\left(-\frac{2^{\frac{R}{f_{sp}(L,K,I)}}-1}{f_s(L,K,I)}\right), \quad (50)$$

according to (25). For $\forall I_1 > I_2, I_1, I_2 \geqslant L-1$, substituting (41) and (46) into (50), *Lemma 1* can be proved due to the monotonic property of the exponential function. ■

In this paper, we aim to determine the optimal MH-ANC scheme, amounting to identifying the number of TTIs for the optimal scheme. The number of TTIs is from $I \in \{2,4,6,...,+\infty\}$, and it is computationally intractable to enumerate the list to determine the optimal TTI. However, *Lemma 1* suggests that the outage probability of I-TTI MH-ANC increases with the number of time intervals when $I > L-1$ for the L-node K-message MH-TRC, meaning that the I-TTI MH-ANC scheme with $I \leqslant L-1$ can achieve better outage performance than those with $I > L-1$. Therefore, the following remark can be intuitively derived from *Lemma 1*.

Remark 1: The number of TTIs for the optimal MH-ANC scheme lies within $\{2,4,...,L-1\}$.

It can be seen that *Remark 1* significantly reduces the computational complexity of searching the number of TTIs for the optimal MH-ANC scheme. In the following section, we will present the outage probabilities of the I-TTI MH-ANC schemes with $I \leqslant L-1$ with the aim of identifying the optimal MH-ANC scheme.

B. Optimal Multi-Hop Analog Network Coding

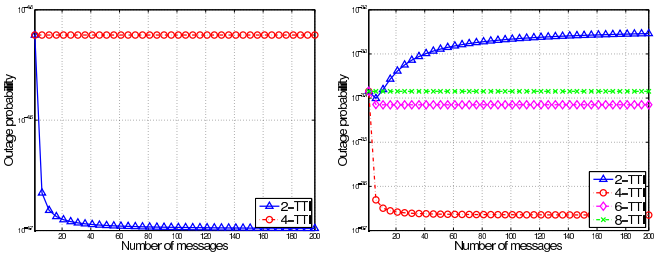

(a) (b)

Fig. 5. Outage probability versus the number of messages for the MH-TRCs of different scales. (a) 5-node MH-TRC. The outage probability for 2-TTI MH-ANC decreases with the number of messages, and the outage probability for 4-TTI MH-ANC remains constant as the outage of early messages does not affect that of later messages; and (b) 9-node MH-TRC. The outage probability of the 2-TTI MH-ANC scheme drops with the increase in the number of messages until a certain value, i.e., $K = 4$, and then rebounds after this value.

Fig. 5 plots the upper bound of the outage probability versus the number of messages. The average SNR per hop is set to 40 dB. It can be found that the outage probability converges to a constant value when the number of messages becomes large. Moreover, 2-TTI MH-ANC has a significantly better outage performance than 4-TTI MH-ANC for the 5-node MH-TRC. Therefore, the optimal MH-ANC scheme for the 5-node MH-TRC is 2-TTI MH-ANC. Similarly, the optimal MH-ANC scheme for the 9-node MH-TRC is 4-TTI MH-ANC.

As can be seen from Fig. 5, the outage probability of the I-TTI MH-ANC scheme reaches a stable value when the number of messages is far larger than the number of nodes. Therefore, we plot the upper bound of the outage probability versus the number of TTIs for the MH-TRCs of different scales with $K = 400$ in Fig. 6. The average SNR per hop is set to 30 dB.

As can be observed from Fig. 6, all the outage probability curves follow almost the same trend, in which the outage probability decreases with the number of TTIs when it is below a certain value, and reaches a valley point, then starts increasing after this valley point. Fig. 6 clearly shows the optimal MH-ANC scheme with the best outage performance for all-scale MH-TRCs. The number of TTIs for the optimal MH-ANC scheme is summarized in Table II.

As can be seen from Table II, the number of TTIs for the optimal MH-ANC scheme generally increases with the number of nodes except for three outliers at $L = 19, 23, 25$. No distinctive patterns for the optimal MH-ANC scheme can be derived from Table II. However, for the outage performance comparison, the upper bound of the outage performance of the optimal MH-ANC and conventional Non-NC schemes are compared in Fig. 7.

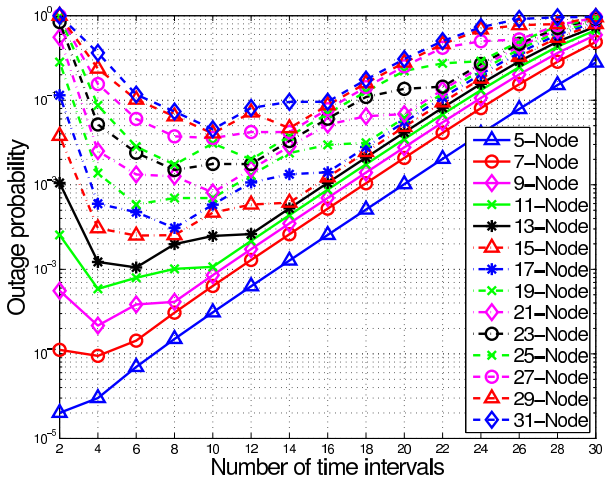

Fig. 6. Outage probability versus the number of TTIs for the MH-TRCs of different scales with $K = 400$.

TABLE II
OPTIMAL MH-ANC SCHEMES FOR THE MH-TRCS OF DIFFERENT SCALES.

Number of nodes (L)	Number of TTIs (I)
5	2
7	4
9	4
11	4
13	6
15	6
17	8
19	6
21	10
23	8
25	8
27	10
29	10
31	10

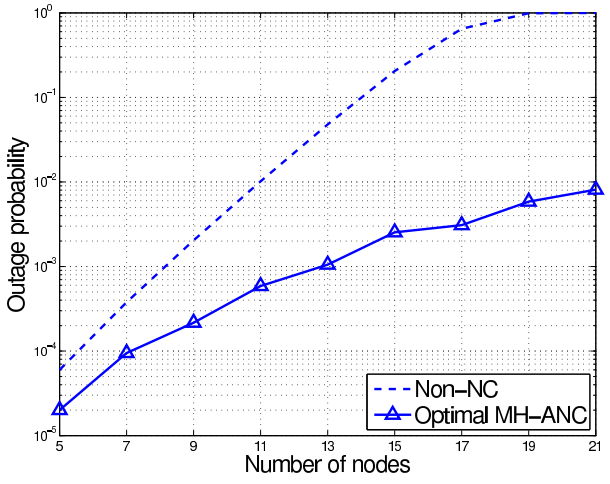

Fig. 7. Outage probability for the optimal MH-ANC scheme versus the number of nodes.

As demonstrated in [16], the outage performance gain of the 2-TTI MH-ANC scheme relative to the Non-NC scheme diminishes when the number of nodes becomes large. However, as can be seen from Fig. 7, the outage probability of the optimal MH-ANC scheme is significantly better than that of the Non-NC scheme, and the gain increases with the number of nodes.

C. Compute-and-Forward Network Coding

In this section, the outage probability of the MH-CPF scheme is derived to determine the relationships with the numbers of nodes, messages, and TTIs, so as to determine the optimal MH-CPF scheme for all-scale MH-TRCs..

Lemma 2: Denoting by $f^o_{\text{MH-CPF}}(L,K,I)$ the outage probability of the L-node K-message MH-TRC with I-TTI MH-ANC, we have

$$f^o_{\text{MH-CPF}}(L,K_1,I) = f^o_{\text{MH-CPF}}(L,K_2,I), \quad \forall K_1,K_2,I \geqslant L-1.$$
$$f^o_{\text{MH-CPF}}(L,K,I_1) < f^o_{\text{MH-CPF}}(L,K,I_2), \quad \forall I_1 > I_2, I_1, I_2 \geqslant L-1.$$

Proof: As inferred from the transmission scheme for I-TTI MH-CPF, when $I \geqslant L-1$, the second outgoing message is transmitted after the first incoming message reaches the user node. There is no inter-message interference, meaning that the transmission of each message does not interfere with each other. Therefore, the outage probability for each message is equivalent to each other, which leads to the first statement in *Lemma 2*.

Moreover, the number of transmission events that affect the transmission of each message remains unchanged with the increase of the number of TTIs when $I \geqslant L-1$. Denote by $\mathcal{F}_{v_k}(L,K,I)$ the set of transmission event that affect the transmission of message v_k, we can obtain

$$\mathcal{F}_{v_k}(L,K,I) \equiv \mathcal{F}_{v_k}(L,K,L-1), \forall I \geqslant L-1. \quad (51)$$

where $\equiv$ stands for identically equal.

On the other hand, the spectral efficiency decreases with the number of nodes, causing the drop of the message rate. As can be seen from (31), when $I \geqslant L-1$, the numbers of components in terms $\mathcal{B}_k$ and $\mathcal{C}_k$ remain unchanged with the number of TTIs, while, the outage probabilities for each component in terms $\mathcal{B}_k$ and $\mathcal{C}_k$ decrease with the increased number of TTIs due to the decrease of the message rate for each transmission. Therefore, terms $\mathcal{B}_k$ and $\mathcal{C}_k$ in (31) decrease with the increased number of TTIs, which proves the second statement in *Lemma 2*. ■

Similar to the situation in MH-ANC, the following remark can be intuitively derived from *Lemma 2* to simplify the identification of the optimal number of TTIs for the MH-CPF scheme.

Remark 2: The number of TTIs for the optimal MH-CPF scheme lies within $\{2,4,...,L-1\}$.

In the following section, only the outage probabilities of the I-TTI MH-CPF schemes with $I \leqslant L-1$ will be presented to identify the optimal MH-CPF scheme.

D. Optimal Compute-and-Forward Network Coding

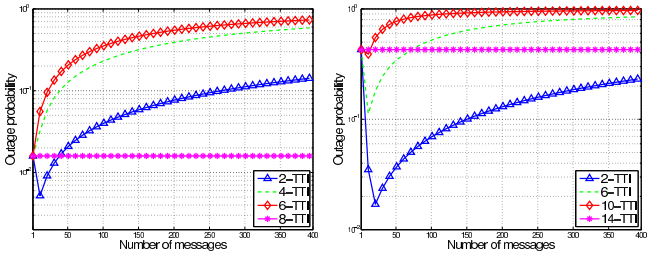

(a) (b)

Fig. 8. Outage probability versus the number of messages for the MH-TRCs of different scales. (a) 9-node MH-TRC. The outage probability for 2-TTI MH-CPF sees a valley point when the number of messages is approximately 6, whilst the other curves with $I < L-1$ increase with the number of messages. The outage probability of 8-TTI MH-CPF remains constant regardless of the number of messages; and (b) 15-node MH-TRC.

Fig. 8 shows the outage probability versus the number of messages. The average SNR per hop is set to 20 dB. It can be clearly seen that the outage probability for I-TTI MH-CPF with $I < L-1$ generally increases with the number of messages. Moreover, when $I = L-1$, the outage probability remains unchanged despite the increased number of messages, as indicated by *Lemma 2*. Fig. 8(a) shows that the outage probability of the $(L-1)$-TTI MH-CPF scheme is larger than the MH-CPF scheme with $I < L-1$ when the number of messages is small. However, the outage probability of the MH-CPF scheme with $I < L-1$ increases quickly with the increase in the number of messages. As a result, the $(L-1)$-TTI MH-CPF scheme has better outage performance than the other schemes when the number of messages is large.

On the other hand, as can be observed from Fig. 8(b), the 2-TTI MH-CPF scheme is always superior to the 14-TTI MH-CPF scheme in the 15-node MH-TRC, when the number of messages is smaller than 400. However, the outage probability of 2-TTI MH-CPF keeps increasing when the number of messages is larger than 400. Therefore, it can be interpreted that the outage probability of 2-TTI MH-CPF will exceed that of 14-TTI MH-CPF when the number of message reaches a certain value (the number is 620 as our experiment results suggest).

Based upon the above discussions, it can be concluded that when the number of messages is relatively small, 2-TTI MH-CPF is the optimal MH-CPF scheme for all-scale MH-TRCs. However, when the number of messages becomes relatively large, the optimal MH-CPF scheme is $(L-1)$-TTI MH-CPF. As an example, we plot the outage probability versus the number of TTIs in Fig. 9 with the number of messages 400.

As can be seen from Fig. 9, all the outage probability curves have a valley point. This point moves rightwards with the increase in the number of nodes. However, the figure also suggests that the valley point is not the lowest outage probability for the MH-TRC with more than 13 nodes, whereas 2-TTI MH-CPF has the lowest outage probability. The figure clearly shows the optimal MH-CPF scheme for all-scale MH-TRCs.

To demonstrate the optimal MH-CPF for different scale

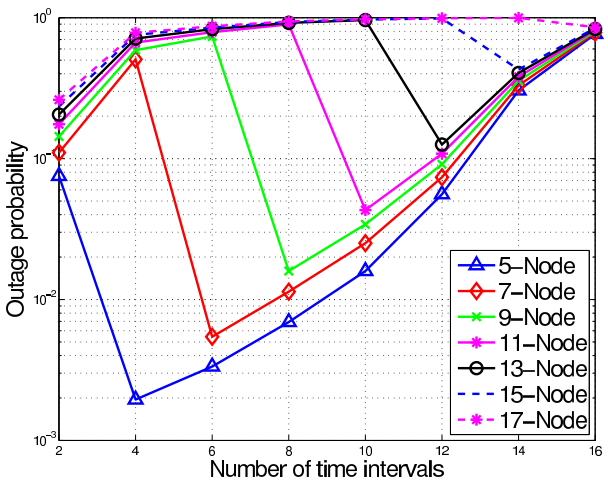

Fig. 9. Outage probability versus the number of TTIs for the MH-TRCs of different scales.

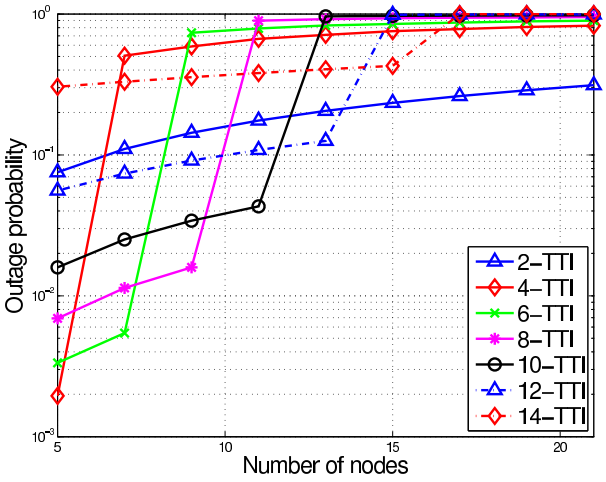

Fig. 10. Outage probability versus the number of nodes for the MH-CPF schemes with different TTIs.

MH-TRCs, the outage probability versus the number of nodes for the MH-CPF scheme with the a variety of TTIs is plotted in Fig. 10. It can be seen from the figure that the outage probabilities for the MH-CPF schemes with different TTIs increase with the number of nodes. Moreover, the outage probability increases steadily with the number of nodes when $I < L-1$, as can be seen from Fig. 10. However, the outage probability of MH-CPF sees a sudden jump when the number of nodes increases from $I+1$ to $I+3$. The figure shows the optimal MH-CPF scheme from a different perspective. That is, when the number of nodes is smaller than 15, the number of TTIs for the optimal MH-CPF scheme is $I = L-1$. However, when the number of nodes is larger than 15, 2-TTI MH-CPF achieves the best outage probability for the MH-TRC.

Fig. 11 plots the outage probabilities of both Non-NC and optimal MH-CPF schemes when the number of messages is 400. The numerical results in [17] showed that 2-TTI MH-CPF can only achieve better outage performance when the number of nodes is relatively large (i.e., $L \geqslant 11$). However,

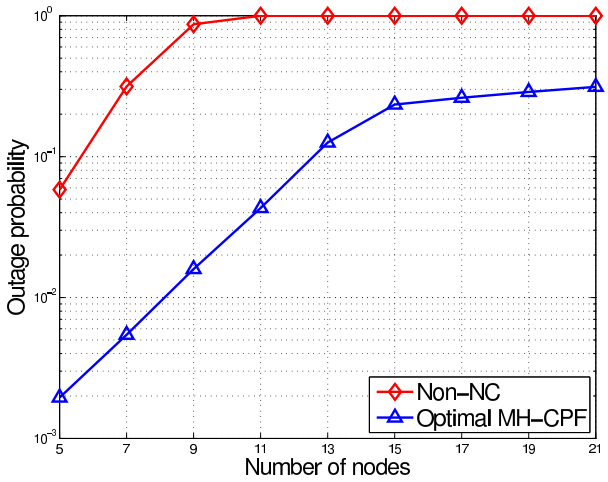

Fig. 11. Outage probability versus the number of nodes for the optimal MH-CPF scheme.

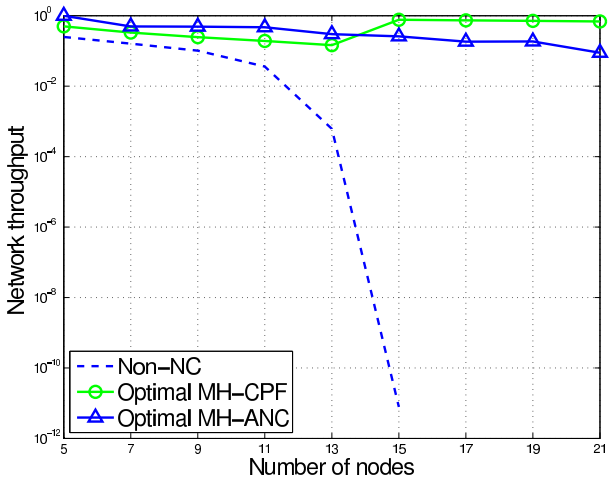

Fig. 12. Network throughput versus the number of nodes.

the optimal MH-CPF scheme has overcome this limitation, achieving a substantially improved outage performance over Non-NC in all-scale MH-TRCs, as shown in Fig. 11.

E. Network Throughput

The network throughput is defined as the number of message successfully exchanged between the two user nodes per time slot [30], given by

$$C \triangleq S(1 - P_f), \tag{52}$$

where P_f is the frame error rate (FER), and S is the spectral efficiency. For fading channels, the analytical expression of FER for MH-WNC is computationally intractable due to the multiple information in the collided signal and random CSI. However, since outage probability P^{out} serves as a lower bound to the frame error rate for block fading environment, in which the channel is constant over a block and is independent from one block to another [31]. Therefore, using bounding technique, the network throughput is upper-bounded as

$$\hat{C} \triangleq S(1 - P^{\text{out}}). \tag{53}$$

Using the upper bound of the outage probability results given in the previous sections, the upper bound of the network throughput versus the number of nodes for the Non-NC, optimal MH-ANC and MH-CPF schemes is shown in Fig. 12.

As can be seen from the above figure, thanks to the spectral efficiency and outage probability advantages, the network throughput of the optimal MH-ANC and MH-CPF schemes are much better than those of the Non-NC schemes.

VI. Conclusion

In this paper, we proposed a generalized I-TTI MH-WNC scheme for the L-node K-message MH-TRC. The transmission scheme is generalized to the MH-WNC scheme with different numbers of TTIs. Network throughput, average received SNR and outage probability are analysed, and closed-form expressions of the outage probability are derived for both MH-ANC and MH-CPF schemes. The numerical results are presented to show the relationships between the numbers of nodes, messages and TTIs with the spectral efficiency, average received SNR, outage probability and network throughput.

It is proven that there exists an optimal MH-WNC scheme for all-scale MH-TRCs. More specifically, for the non-regenerative MH-TRC, the number of TTIs of the optimal MH-ANC scheme generally increases with the number of nodes. It is also shown that the outage performance of the optimal MH-ANC scheme has significantly better outage performance than Non-NC in all-scale MH-TRCs, and the outage probability gain increases with the number of nodes.

For the regenerative MH-TRC with a relatively small number of messages, the optimal MH-CPF scheme is the 2-TTI MH-CPF scheme. On the other hand, the $(L-1)$-TTI MH-CPF scheme is the optimal MH-CPF scheme when the number of messages is large enough. It is also proven that the optimal MH-CPF scheme is able to outperform the Non-NC scheme in all-scale MH-TRCs.

Moreover, thanks to the spectral efficiency and outage probability advantages, the network throughput of the optimal MH-ANC and MH-CPF schemes are much better than those of the Non-NC schemes.

Acknowledgment

This work was supported in part by the National Basic Research Program of China under grant of 61201179.

Appendix A
Received SNR Derivation for message v_1 in the 5-node 2-message MH-TRC with 2-TTI MH-ANC

Since only some transmission events affect the noise propagation, the transmission matrix for each message can be further converted into a characteristic matrix that only contains the affected transmission events. Hence, the characteristic matrix

of v_1 can be obtained by removing the last two rows of matrix $\mathbf{T}_{5,2}^2$ in (2) and setting unaffected event elements to zero as

$$\mathbf{T}_{v_1} = \begin{bmatrix} 1 & -1 & 0 & -1 & 1 \\ 0 & 1 & -2 & 1 & 0 \\ 1 & -2 & 1 & 0 & 0 \\ -1 & 1 & 0 & 0 & 0 \end{bmatrix}. \tag{54}$$

Furthermore, it can be found that only four transmission events in characteristic matrix $\mathbf{T}_{v_1}$ affect the noise propagation, i.e., N_2 to N_3 (element (2,2)), N_4 to N_3 (element (2,4)), N_3 to N_2 (element (3,3)), and N_2 to N_1 (element (4,2)). Therefore, the noise matrix of $\mathbf{T}_{v_1}$ can be represented as

$$\mathbf{N}_{v_1} = \begin{bmatrix} 0 & 0 & 0 & 0 & 0 \\ 0 & 1 & 0 & 2 & 0 \\ 0 & 0 & 3 & 0 & 0 \\ 0 & 3 & 0 & 0 & 0 \end{bmatrix}, \tag{55}$$

where "1" represents the single access transmission to right neighboring node with weight W_l^1, "2" represents the single access transmission to the left neighboring node with weight W_l^2, and "3" represents the broadcast transmission to both neighboring nodes with weight W_l^3,

Corresponding to the three types of weights, the above noise matrix can be further divided into three sub-noise matrices. For example, the noise matrix given by (55) can be decomposed into $\mathbf{N}_{v_1}^i, i \in \{1,2,3\}$ as

$$\mathbf{N}_{v_1}^1 = \begin{bmatrix} 0&0&0&0&0 \\ 0&1&0&0&0 \\ 0&0&0&0&0 \\ 0&0&0&0&0 \end{bmatrix}, \mathbf{N}_{v_1}^2 = \begin{bmatrix} 0&0&0&0&0 \\ 0&0&0&1&0 \\ 0&0&0&0&0 \\ 0&0&0&0&0 \end{bmatrix}, \mathbf{N}_{v_1}^3 = \begin{bmatrix} 0&0&0&0&0 \\ 0&0&0&0&0 \\ 0&0&1&0&0 \\ 0&1&0&0&0 \end{bmatrix}.$$

Substituting the weight at each node into the above three matrices, the noise power matrix containing the weights of each transmission that affect the transmission of v_1 can be computed as

$$\begin{aligned} \tilde{\mathbf{N}}_{v_1} &= \sum_{i=1}^{3} \left(\mathbf{N}_{v_1}^i \circ \mathbf{W}^i \right) \\ &= \mathbf{N}_{v_1}^1 \circ \mathbf{W}^1 + \mathbf{N}_{v_1}^2 \circ \mathbf{W}^2 + \mathbf{N}_{v_1}^3 \circ \mathbf{W}^3 \\ &= \begin{bmatrix} 0&0&0&0&0 \\ 0&W_2^1&0&0&0 \\ 0&0&0&0&0 \\ 0&0&0&0&0 \end{bmatrix} + \begin{bmatrix} 0&0&0&0&0 \\ 0&0&0&W_4^2&0 \\ 0&0&0&0&0 \\ 0&0&0&0&0 \end{bmatrix} + \begin{bmatrix} 0&0&0&0&0 \\ 0&0&0&0&0 \\ 0&0&W_3^3&0&0 \\ 0&W_2^3&0&0&0 \end{bmatrix} \\ &= \begin{bmatrix} 0&0&0&0&0 \\ 0&W_2^1&0&W_4^2&0 \\ 0&0&W_3^3&0&0 \\ 0&W_2^3&0&0&0 \end{bmatrix}. \end{aligned} \tag{56}$$

In high SNR regions, the upper bound of the noise power matrix of message v_1 in the 5-node 3-message MH-TRC with 2-TTI MH-ANC can be obtained using (16) as

$$\tilde{\mathbf{N}}_{v_1} = \begin{bmatrix} 0 & 0 & 0 & 0 & 0 \\ 0 & 0.7500 & 0 & 0.7500 & 0 \\ 0 & 0 & 0.6667 & 0 & 0 \\ 0 & 0.3750 & 0 & 0 & 0 \end{bmatrix}, \tag{57}$$

and the noise power can be calculated by traversing the noise power matrix as

$$\mathcal{N}_{\text{MH-ANC},v_1} = 6.33\sigma^2, \tag{58}$$

Similarly, the signal matrix contains only the transmission events that affect the propagation of the signal power. The signal matrix of message v_1 for the 5-node 2-message MH-TRC can be obtained as

$$\tilde{\mathbf{S}}_{v_1} = \begin{bmatrix} 0 & 0 & 0 & 0 & 4 \\ 0 & 0 & 0 & 2 & 0 \\ 0 & 0 & 3 & 0 & 0 \\ 0 & 3 & 0 & 0 & 0 \end{bmatrix}. \tag{59}$$

where elements "1", "2" and "3" represent the same events as defined in the noise matrix, and "4" represents the transmission at the user nodes N_1 and N_L, where the corresponding weight $W_l^4 = P_l|h|^2$. Thus, the signal power matrix can be similarly obtained as

$$\begin{aligned} \tilde{\mathbf{S}}_{v_1} &= \sum_{i=1}^{4} \left(\mathbf{S}_{v_1}^i \circ \mathbf{W}^i \right) \\ &= \mathbf{S}_{v_1}^1 \circ \mathbf{W}^1 + \mathbf{S}_{v_1}^2 \circ \mathbf{W}^2 + \mathbf{S}_{v_1}^3 \circ \mathbf{W}^3 + \mathbf{S}_{v_1}^4 \circ \mathbf{W}^4 \\ &= \begin{bmatrix} 0&0&0&0&0 \\ 0&0&0&W_4^2&0 \\ 0&0&0&0&0 \\ 0&0&0&0&0 \end{bmatrix} + \begin{bmatrix} 0&0&0&0&0 \\ 0&0&0&0&0 \\ 0&0&W_3^3&0&0 \\ 0&W_2^3&0&0&0 \end{bmatrix} + \begin{bmatrix} 0&0&0&0&W_5^4 \\ 0&0&0&0&0 \\ 0&0&0&0&0 \\ 0&0&0&0&0 \end{bmatrix} \\ &= \begin{bmatrix} 0&0&0&0&W_5^4 \\ 0&0&0&W_4^2&0 \\ 0&0&W_3^3&0&0 \\ 0&W_2^3&0&0&0 \end{bmatrix}. \end{aligned} \tag{60}$$

Similarly, in high SNR regions, the signal power matrix for message v_1 in the 5-node 3-message MH-TRC with 2-TTI MH-ANC can be obtained as

$$\tilde{\mathbf{S}}_{v_1} = \begin{bmatrix} 0 & 0 & 0 & 0 & 2P|h|^2 \\ 0 & 0 & 0 & 0.7500 & 0 \\ 0 & 0 & 0.6667 & 0 & 0 \\ 0 & 0.3750 & 0 & 0 & 0 \end{bmatrix}. \tag{61}$$

and the signal power is

$$\mathcal{S}_{\text{MH-ANC},v_1} = 0.38P|h|^2, \tag{62}$$

Thus, an upper bound of the received SNR of message v_1 in the 5-node 3-message MH-TRC with 2-TTI MH-ANC can be obtained as

$$\hat{\gamma}_{\text{MH-ANC},v_1} = \frac{0.38P|h|^2}{6.33\sigma^2} = 0.06P\gamma', \tag{63}$$

where $\gamma' = \frac{|h|^2}{\sigma^2}$ is the average SNR of each hop.

REFERENCES

[1] I. F. Akyildiz, W. Su, Y. Sankarasubramaniam, and E. Cayirci, "A survey on sensor networks," *IEEE Commun. Mag.*, vol. 40, pp. 102 – 114, Aug. 2002.

[2] I. F. Akyildiz and X. Wang, "A survey on wireless mesh networks," *IEEE Commun. Mag.*, vol. 43, pp. 23 – 30, Sep. 2005.

[3] T. Camp, J. Boleng, and V. Davies, "A survey of mobility models for ad hoc network research," *Wireless Communications & Mobile Computing: Special issue on Mobile Ad Hoc Networking: Research, Trends and Applications*, vol. 2, pp. 483 – 502, Sep. 2002.

[4] H. Hartenstein and K. Laberteaux, "A tutorial survey on vehicular ad hoc networks," *IEEE Commun. Mag.*, vol. 46, pp. 164 – 171, Jun. 2008.

[5] H. Ju, E. Oh, and D. Hong, "Catching resource-devouring worms in next-generation wireless relay systems: Two-way relay and full-duplex relay," *IEEE Commun. Mag.*, vol. 47, pp. 58 – 65, Sep. 2009.

[6] K. Zheng, F. Liu, L. Lei, C. Lin, and Y. Jiang, "Stochastic performance analysis of a wireless finite-state markov channel," *IEEE Trans. Wireless Commun.*, vol. 12, pp. 782 – 793, Feb. 2013.

[7] R. Ahlswede, N. Cai, S.-Y. Li, and R. Yeung, "Network information flow," *IEEE Trans. Inform. Theory*, vol. 47, pp. 1204 – 1216, Jul. 2000.

[8] S. Zhang, S. C. Liew, and P. P. Lam, "Hot topic: physical-layer network coding," in *Proc. International conference on Mobile computing and networking*, Los Angeles, CA, Sep. 2006, pp. 23 – 29.

[9] S. Katti, H. Rahul, W. Hu, D. Katabi, M. Medard, and J. Crowcroft, "XORs in the air: Practical wireless network coding," *IEEE/ACM Trans. Networking*, vol. 21, pp. 497–510, Mar. 2008.

[10] M. Ju and I.-M. Kim, "Error performance analysis of BPSK modulation in physical-layer network-coded bidirectional relay networks," *IEEE Trans. Commun.*, vol. 58, pp. 2770 – 2775, Oct. 2010.

[11] R. Louie, Y. Li, and B. Vucetic, "Practical physical layer network coding for two-way relay channels: performance analysis and comparison," *IEEE Trans. Wireless Commun.*, vol. 9, pp. 764 – 777, Feb. 2010.

[12] M. Park, I. Choi, and I. Lee, "Exact BER analysis of physical layer network coding for two-way relay channels," in *Proc. IEEE Vehicular Technology Conference (VTC Spring)*, Budapest, Hungary, May 2011, pp. 1 – 5.

[13] S. Zhang, S. C. Liew, and L. Lu, "Physical layer network coding schemes over finite and infinite fields," in *Proc. IEEE Global Telecommunications Conference*, New Orleans, LA, Nov. 2008, p. 1.

[14] Q. You, Z. Chen, Y. Li, and B. Vucetic, "Multi-hop bi-directional relay transmission schemes using amplify-and-forward and analog network coding," in *Proc. IEEE International Conference on Communications*, Kyoto, Japan, Jun. 2011, pp. 1 – 6.

[15] Q. You, Z. Chen, and Y. Li, "A multihop transmission scheme with detect-and-forward protocol and network coding in two-way relay fading channels," *IEEE Trans. Veh. Technol.*, vol. 61, pp. 433 – 438, Jan. 2012.

[16] G. Wang, W. Xiang, J. Yuan, and T. Huang, "Outage analysis of non-regenerative analog network coding for two-way multi-hop networks," *IEEE Commun. Lett.*, vol. 15, pp. 662 – 664, May 2011.

[17] G. Wang, W. Xiang, and J. Yuan, "Multi-hop compute-and-forward for generalized two-way relay channels," *Transactions on Emerging Telecommunications Technologies, available at http://onlinelibrary.wiley.com/doi/10.1002/ett.2644/full*.

[18] G. Wang, W. Xiang, J. Yuan, and T. Huang, "Outage performance of analog network coding in generalized two-way multi-hop networks," in *Proc. IEEE Wireless Communications and Networking Conference*, Cancun, Quintana Roo, Mar. 2011, pp. 1988 – 1993.

[19] K. Lee, W. Sung, and J. W. Jang, "Application of network coding to IEEE 802.16j mobile multi-hop relay network for throughput enhancement," *Journal of Communications and Networks*, vol. 10, no. 4, pp. 412–421, 2008.

[20] M. O. Hasna and M. S. Alouini, "Harmonic mean and end-to-end performance of transmission systems with relays," *IEEE Trans. Commun.*, vol. 52, pp. 130 – 135, Jan. 2004.

[21] M. Hasna and M.-S. Alouini, "Outage probability of multihop transmission over Nakagami fading channels," *IEEE Commun. Lett.*, vol. 7, pp. 216 – 218, May 2003.

[22] Y. Li, B. Vucetic, Z. Chen, and J. Yuan, "An improved relay selection scheme with hybrid relaying protocols," in *Proc. IEEE GLOBECOM*, Washington, DC, Nov. 2007, pp. 3704 – 3708.

[23] E. Morgado, I. Mora-Jimenez, J. Vinagre, J. Ramos, and A. Caamano, "End-to-end average BER in multihop wireless networks over fading channels," *IEEE Trans. Wireless Commun.*, vol. 9, pp. 2478 – 2487, Jul. 2010.

[24] B. Nazer and M. Gastpar, "Reliable physical layer network coding," *Proceedings of the IEEE*, vol. 99, pp. 438 – 460, Mar. 2011.

[25] ——, "Compute-and-forward: Harnessing interference throught strucutred codes," *IEEE Trans. Inform. Theory*, vol. 57, pp. 6463 – 6486, Oct. 2011.

[26] T. Yang, T. Huang, J. Yuan, and Z. Chen, "Distance spectrum and performance of channel-coded physical-layer network coding for binary-input gaussian two-way relay channels," *IEEE Trans. Commun.*, vol. 60, pp. 1499 – 1510, Jun. 2012.

[27] A. Osmane and J.-C. Belfiore, "The compute-and-forward protocol: Implementation and practical aspects," *submitted to IEEE Communication Letters*.

[28] C. Feng, D. Silva, and F. Kschischang, "Design criteria for lattice network coding," in *Proc. Annual Conference on Information Sciences and Systems*, Baltimore, MD, Mar. 2011, pp. 1 – 6.

[29] H. Yao and G. Wornell, "Lattice-reduction-aided detectors for MIMO communication systems," in *Proc. IEEE Global Commun. Conf.*, Taipei, Taiwan, R.O.C., Nov. 2002, pp. 424 – 428.

[30] A. Goldsmith, *Wireless Communications*. New York: Cambridge, 2005.

[31] L. Ozarow, S. Shamai, and A. Wyner, "Information theoretic considerations for cellular mobile radio," *IEEE Trans. Veh. Technol.*, vol. 43, pp. 359 – 378, Feb. 1994.